Hybrid temporal LES: Development and applications

Remi Manceau

Hybrid temporal LES: Development and applications

Rémi Manceau

CNRS / Univ Pau & Pays Adour / E2S UPPA
Laboratoire de mathématiques et de leurs applications de Pau
Fédération IPRA, UMR 5142, 64000, Pau, France
and Inria Bordeaux-Sud-Ouest, project-team CAGIRE

Abstract

The HTLES approach, based on temporal filtering, is a formally consistent way to hybridize (U)RANS and LES. Recent advances are presented as well as applications using industrial codes, which show the strong potential of this approach for industrial CFD.

1 Introduction

A rigorous formalism for continuous hybrid RANS/LES methods is highly desirable to favour the modelling of subgrid stresses, comparison with experiments/DNS and understanding of the observed phenomenology. The usual hybrid methods are limited by the fact that statistical averaging (RANS) and spatial filtering (LES) are generally inconsistent [1].

1.1 Temporal filtering

Generalized temporal filters, characterized by time integration at a moving application point,

$$\widetilde{\mathbf{U}}(\mathbf{x},t) = \int_{-\infty}^{t} G_T(t,t')\mathbf{U}(\boldsymbol{\xi}(\mathbf{x},t,t'),t')\,\mathrm{d}t', \quad (1)$$

are introduced in order to build a consistent formalism for hybrid methods for stationary, inhomogeneous turbulence, since the time-filtered quantities go to the statically-averaged quantities within the limit of an infinite filter width [1]. To satisfy the Galilean invariance, the *uniform temporal filter* [2] is used here,

$$\boldsymbol{\xi}(\mathbf{x},t,t') = \mathbf{x} + (t'-t)\mathbf{V}_{\mathrm{ref}}, \quad (2)$$

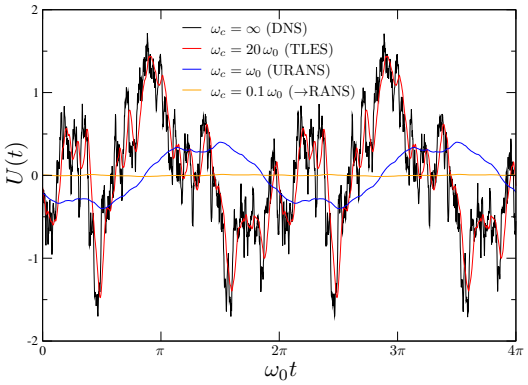

Figure 1: Synthetic turbulent signal. Application of a top-hat temporal filter with several cutoff frequencies ω_c. ω_0 corresponds to the integral scale.

where $\mathbf{V}_{\mathrm{ref}}$ is an arbitrary velocity. As illustrated by Figure (1), the filtering process leads to temporal LES (TLES), URANS or RANS, depending on the cut-off frequency. The phase shift is due to backward-in-time integration (causal filter).

The equation of the filtered momentum is as follows

$$\frac{\partial \widetilde{U}_i}{\partial t} + \widetilde{U}_k \frac{\partial \widetilde{U}_i}{\partial x_k} = -\frac{1}{\rho}\frac{\partial \widetilde{P}}{\partial x_i} + \nu \frac{\partial^2 \widetilde{U}_i}{\partial x_j \partial x_j} - \frac{\partial \tau_{ij_{\mathrm{sfs}}}}{\partial x_j} \quad (3)$$

and the transport equation for the subfilter stress (SFS) tensor $\tau_{ij_{\mathrm{sfs}}}$ is also formally identical to the RANS equation for the Reynolds-stress tensor $\overline{u_i u_j}$, and tends exactly towards this equation within the limit of an infinite filter width, which forms a solid foundation for the development of hybrid RANS/LES approaches [1].

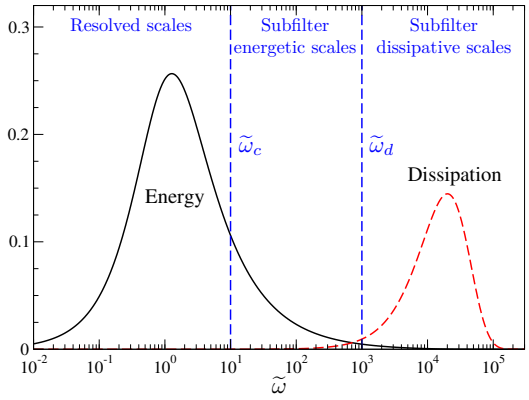

Figure 2: Spectral zones of HTLES. Premultiplied energy and dissipation spectra, $\widetilde{\omega}\widetilde{E}(\widetilde{\omega})$ and $\widetilde{\omega}\widetilde{D}(\widetilde{\omega})$, respectively, in units based on the integral scales.

1.2 Hybridrization with URANS

For a filter width of the order of magnitude of the integral time scale of turbulence, the filtered velocity only contains large-scale, quasi-periodic oscillations, Figure (1), similar to URANS solutions. It can be shown that using this filter width leads to the URANS equations (i.e., the RANS system with time derivative) such that URANS can be regarded as a time-filtered approach [2]. As a consequence, the HTLES methodology can also be used to bridge URANS and Temporal LES, which extends the validity of HTLES to non-stationary configurations.

2 Subfilter stress model

As in the case of standard LES, a closure problem must be addressed due to the presence of the subfilter stresses $\tau_{ij_{\mathrm{sfs}}}$ in Eq. (3).

2.1 Hybridization method

The HTLES approach is based on the introduction of two filters with characteristic frequencies ω_c and ω_d, Figure (2). Integrating the equation for the *Eulerian temporal energy spectrum* $E_T(\mathbf{x},\omega)$ on the ranges $[\omega_c;\omega_d]$ and $[\omega_d;\infty[$, respectively [1], and using a perturbation method to derive the dissipation term [3], the equation for the subfilter turbulent energy k_{sfs} can be written as follows

$$\frac{\mathrm{D}k_{\mathrm{sfs}}}{\mathrm{D}t} = P_{\mathrm{sfs}} + D_{\mathrm{sfs}} - \frac{k_{\mathrm{sfs}}}{T}, \tag{4}$$

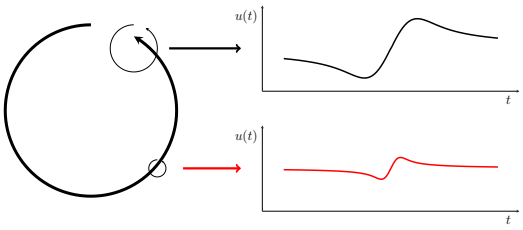

Figure 3: Sweeping mechanism [7].

where P_{sfs} and D_{sfs} are the subfilter parts of production and diffusion. The time scale that determines the dissipation term is

$$T(r) = \frac{r}{\psi(r)}\frac{k}{\varepsilon}, \tag{5}$$

where

$$r = \frac{\overline{k_{\mathrm{sfs}}}}{k} \quad ; \quad \psi(r) = 1 + \left(\frac{C_{\varepsilon 2}}{C_{\varepsilon 1}} - 1\right)\left(1 - r^{\frac{C_{\varepsilon 1}}{C_{\varepsilon 2}}}\right) \tag{6}$$

(the overbar denotes Reynolds averaging). The subfilter-to-total turbulent energy ratio r goes to unity at the RANS limit, in which case Eq. (4) tends towards the RANS equation. The modified time scale enforces the LES mode for $r < 1$ by increasing the dissipation term k_{sfs}/T, similar to two-equation DES. This method can be applied to two-equation models ([4, 5, 6] or to second moment closures, replacing ε in the dissipation tensor with k_{sfs}/T [3]. Eq. (4) bears similarities with the corresponding equation in DES, in which the dissipation term writes $k_{\mathrm{sfs}}^{3/2}/L$. However, HTLES also differs significantly from DES: it relies on a modified time scale rather than a length scale; Eq. (5) is based on the comparison of averaged quantities (r and k/ε); DES is an empirical approach, without explicit reference to a particular formalism, although it can be interpreted as a simplified version of HTLES [3].

2.2 Switchover criterion

As seen in Eq. (5), the criterion that determines the switchover from RANS to LES is the ratio r, which must now be linked to the cutoff frequency ω_c. It seems optimal to link the cutoff frequency to the Nyquist frequency related to the time step dt,

$$\omega_c = \frac{2\pi}{2dt}. \tag{7}$$

However, for a sufficiently small time step, this frequency cannot be observed in the computation,

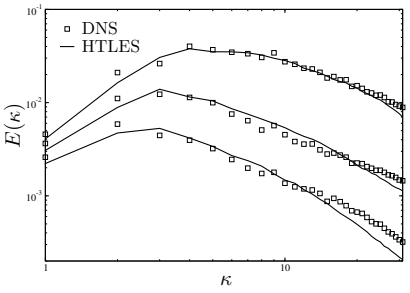

Figure 4: Decaying isotropic turbulence at $Re_\lambda = 104.5$. Evolution over time of the energy spectrum predicted by HTLES based on the k-ω-SST model [4].

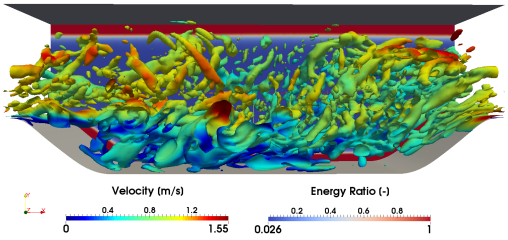

Figure 5: Hill flow. Q-isosurfaces coloured by the velocity magnitude. Background : ratio r_s [6].

since the corresponding vortices are filtered out by the grid. Frequencies observed at a fixed point are related to the advection (sweeping) of small scales by large scales [7], Figure (3). The medium-size vortex at the top is swept by the large-scale structure, so that it generates the time-dependent signal at a fixed point shown in the figure at the top right. The small vortex at the bottom generates higher frequencies. However, if the grid is not fine enough, small vortices and their corresponding frequencies are missing, so the maximum observable frequency is

$$\omega_c = \min\left(\frac{\pi}{dt}; \frac{U_s \pi}{\Delta}\right) = \frac{U_s \pi}{\Delta} \min\left(1; \frac{\Delta}{U_s dt}\right), \tag{8}$$

where U_s is the sweeping velocity [7], and $U_s dt/\Delta$ can be called *the sweeping CFL number*. The sweeping velocity is $U_s = U + u$, where U is the mean velocity magnitude and $u = \gamma\sqrt{k}$ is the characteristic velocity of the energetic eddies, with γ a coefficient usually chosen as unity.

The assumption of an equilibrium Eulerian spectrum [7]

$$E_T(\omega) = C_\kappa \varepsilon^{2/3} U_s^{2/3} \omega^{-5/3}, \tag{9}$$

yields

$$r = \frac{1}{k}\int_{\omega_c}^{\infty} E_T(\omega)\,\mathrm{d}\omega = \frac{1}{\beta}\left(\frac{U_s}{\sqrt{k}}\right)^{2/3}\left(\omega_c \frac{k}{\varepsilon}\right)^{-2/3} \tag{10}$$

As usual for hybrid RANS/LES methods, the coefficient $\beta = 0.67$ is calibrated in homogeneous isotropic turbulence, so that, as shown in Figure (4), the decay of energy follows the DNS data.

Note that Eq. (10) and Eq. (8) actually define a twofold switchover criterion: if the sweeping CFL number is less than one, the switchover criterion is the ratio of the grid step to the integral length scale; otherwise, it is the ratio of the time step to the integral time scale.

2.3 Shielding of the near-wall region

One of the main objectives of hybrid approaches is to treat the near-wall region in RANS mode, in order to avoid the unaffordable cost of wall-resolved LES. Fadai-Ghotbi *et al.* [8] proposed to shield the near-wall region, an idea that was developed independently for the DDES approach [9]. In order to define a shielding function independent of the grid, it is important to base its definition on quantities that are the same in both RANS and LES modes. Duffal *et al.* [6] replaced in Eq. (5) and Eq. (6) the ratio r by the shielded ratio r_s

$$r_s = 1 - f_s \max[0, 1 - r], \tag{11}$$

with the shielding function f_s

$$f_s = 1 - \tanh\left[\xi^p\right] \text{ where } \xi = C_L \frac{\left(\nu^3/\varepsilon\right)^{1/4}}{d_w}, \tag{12}$$

and d_w is the distance to the wall. The advantage of using the Kolmogorov scale in ξ rather than, for example, the integral scale, is that the dissipation rate ε, obtained from its transport equation, is reasonably independent of the grid, such that the thickness of the shielded region is also grid-independent [6].

Another possibility is to use the elliptic-blending parameter α [8, 5], solution of

$$\alpha - L_{\mathrm{sfs}}^2 \nabla^2 \alpha = 1, \tag{13}$$

with $\alpha = 0$ at the wall and define r_s as

$$r_s = (1 - \alpha^2) + \alpha^2 r. \tag{14}$$

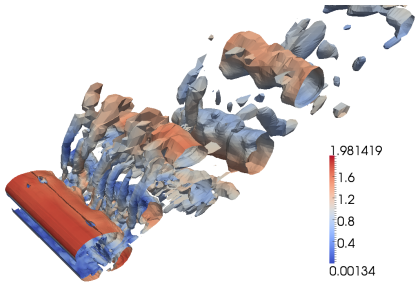

Figure 6: Square-sectioned cylinder. Q-isosurfaces coloured by the velocity magnitude [10].

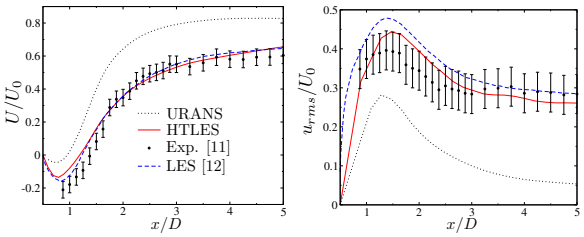

Figure 7: Square-sectioned cylinder. Mean (left) and rms (right) streamwise velocities along the axis of symmetry.

Another difficulty is that the shielding does not prevent resolved vortices from penetrating into the near-wall RANS region, Figure (5). In order to avoid double-counting, Duffal *et al.* [6] proposed the internal consistency constraint (ICC), which excludes the resolved energy k_r due to these fluctuations from the total turbulent energy by the use of

$$T = \frac{r}{\psi(r)} \frac{\overline{k_{\text{sfs}}} + c_r k_r}{\varepsilon}, \text{ where } c_r = \begin{cases} 0 & \text{if } r_s = 1, \\ f_s & \text{if } r_s < 1. \end{cases} \quad (15)$$

3 Some Applications

3.1 Square-sectioned cylinder

To illustrate the predictive capabilities of the method, the first case is the flow around a square-sectioned cylinder at $Re = 21400$, computed using Code_Saturne [4]. Figure (6) shows that the flow in the vicinity of the cylinder is smooth and quasi-2D as in URANS computations. In the wake, the model gradually switches to the LES mode.

Figure (7) shows profiles extracted along the symmetry line behind the cylinder. URANS and HTLES are using the same closure, the k-ω-SST model, and the same grid. This figure clearly shows the superiority of HTLES over URANS. The HTLES results are also close to the LES results, although the number of cells is reduced by a factor of 145 (0.5×10^6 vs. 72.9×10^6), because the near-wall region is resolved in URANS mode.

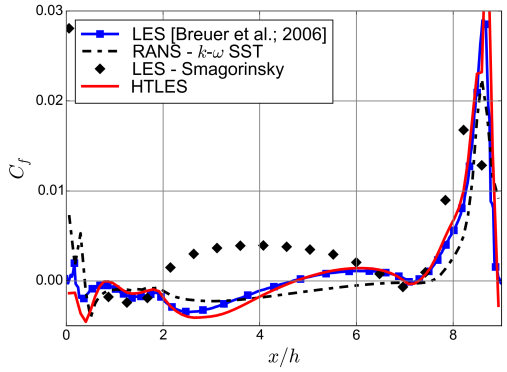

Figure 8: Hill flow. Distribution of skin friction on the lower wall [6].

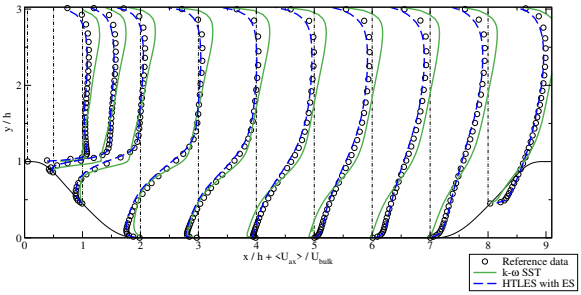

Figure 9: Hill flow. Streamwise velocity profiles. From Afailal *et al.* [5].

3.2 Periodic-Hill Flow

The second case is the periodic hill [13] at $Re_b = 10600$. Computations are performed with Code_Saturne [6], using the hybridized k-ω-SST model. Figure (5) displays in the background the ratio r, which indicates that the hybrid model operates in RANS mode close to the two walls and in LES mode elsewhere.

The skin friction coefficient, Figure (8), is quite well reproduced compared to the results of the refined LES [13], although the number of grid cells in reduced by a factor of 70. RANS, using the same k-ω-SST closure, is not able to reproduce the correct reattachment length. LES, using the same mesh as for HTLES does not give acceptable

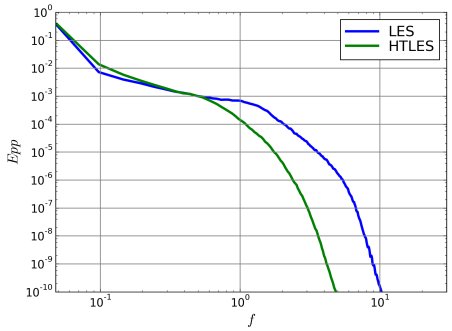

Figure 10: Hill flow. Pressure spectrum at the top of the hill [6].

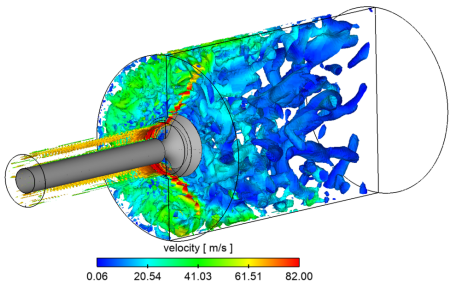

Figure 11: Steady flow rig. HTLES computation. Q-isosurfaces coloured by the velocity magnitude. Only half of the cylinder is shown. From Afailal *et al.* [5].

results, which shows the importance of switching to RANS close to the wall. The same conclusion was reached by Afailal *et al.* [5] using a different CFD code, *Converge CFD*: Figure (9) shows the drastic improvement of the velocity profiles.

Another particularly interesting point is that, as shown in Figure (10), HTLES is able to provide information on wall pressure fluctuations at the wall at a CPU cost much lower than LES, with the exception of the highest frequencies, which can be very useful for predicting of unsteady pressure loads and mechanical fatigue in industrial applications.

3.3 Steady flow rig

The third case is called the *steady flow rig* [14], Figure (11), which is a simplified in-cylinder flow around a valve with a fixed lift at $Re_b = 30000$, computed using Converge CFD [5]. It can be seen in Figure (12) that RANS does not correctly reproduce the black-flow and the radial velocity. On the other hand, HTLES provides results similar to those of LES and is in relatively good agreement with the experiments.

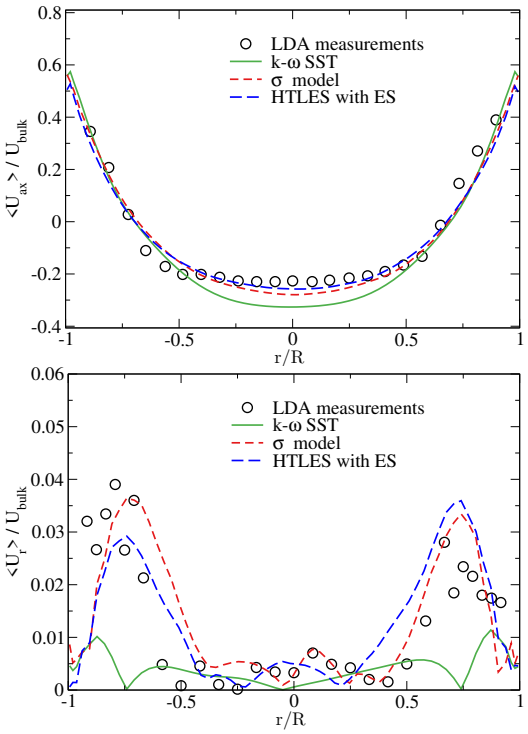

Figure 12: Steady flow rig. Velocity along a radial line located $5.8D$ downstream the expansion. Top: axial component. Bottom: radial component. From Afailal *et al.* [5].

But the most interesting result in favour of the hybrid model is the prediction of the pressure drop given in Table (1). The success of HTLES in this matter compared to LES relies on the use of the RANS mode in the admission pipe and around the valve, where a refined LES would be necessary. This result is probably the best illustration of the main asset of hybrid methods in general, and HTLES in particular: the use of the most appropriate model in each region of the flow.

4 Conclusion

Temporal filtering provides a consistent formalism for the hybridization of RANS (or URANS) and LES, either for first or second moment closures. The resulting HTLES approach bears some similarities with DES, but migrates from RANS to

	EXP	RANS	HTLES	LES
ΔP [Pa]	1766	1713	1705	1957
Error [%]		-3	-3	+11

Table 1: Steady flow rig. Pressure drop between the inlet pipe and the outlet of the domain [5].

LES in a very different way. Recent applications have demonstrated the performance of HTLES, which is able to provide results similar to those of LES, with a drastic cost reduction linked to the use of RANS in the near-wall region. These results also show the potential of hybrid approaches for the prediction of unsteady loads and as a solution to the issue of the prediction of the pressure drop with LES in industrial applications.

Acknowledgements

Several colleagues and students have contributed over the years to the progress of time-filtered hybrid RANS/LES approaches. They are listed in alphabetical order: H. Afailal, Ch. Angelberger, J. Borée, V. Duffal, A. Fadai-Ghotbi, Ch. Friess, J. Galpin, T.B. Gatski, B. de Laage de Meux, R. Perrin, T.T. Tran, A. Velghe. The author is indebted to T.T. Tran, V. Duffal and H. Afailal for producing the results and figures presented in section 3. A part of this work was supported by ANR within the framework of the MONACO_2025 project (ANR-17-CE06-0005-01 ACT).

References

[1] A. Fadai-Ghotbi, C. Friess, R. Manceau, T. Gatski, and J. Borée, "Temporal filtering: a consistent formalism for seamless hybrid RANS-LES modeling in inhomogeneous turbulence," *Int. J. Heat Fluid Fl.*, vol. 31, no. 3, pp. 378–389, 2010.

[2] R. Manceau, "Progress in Hybrid Temporal LES," vol. 137 of *Notes on Numerical Fluid Mechanics and Multidisciplinary Design*, pp. 9–25, Springer, 2018.

[3] C. Friess, R. Manceau, and T. Gatski, "Toward an equivalence criterion for hybrid RANS/LES methods," *Comput. Fluids*, vol. 122, pp. 233–246, 2015.

[4] T. Tran, R. Manceau, R. Perrin, J. Borée, and A. Nguyen, "A hybrid temporal LES approach. Application to flows around rectangular cylinders," in *Proc. 9th ERCOFTAC Int. Symp. on Eng. Turb. Modelling and Measurements, Thessaloniki, Greece*, 2012.

[5] H. Afailal, J. Galpin, A. Velghe, and R. Manceau, "Development and validation of a hybrid temporal LES model in the perspective of applications to internal combustion engines," *Oil Gas Sci. Technol.*, vol. 74, no. 56, p. 16, 2019.

[6] V. Duffal, B. de Laage de Meux, and R. Manceau, "Development and validation of a hybrid RANS/LES approach based on temporal filtering," in *Proc. ASME-JSME-KSME Joint Fluids Eng. Conf. 2019, San Francisco, CA, USA*, 2019.

[7] H. Tennekes, "Eulerian and Lagrangian time microscales in isotropic turbulence," *J. Fluid Mech.*, vol. 67, pp. 561–567, 1975.

[8] A. Fadai-Ghotbi, R. Manceau, and J. Borée, "A seamless hybrid RANS/LES model based on transport equations for the subgrid stresses and elliptic blending," in *Proc. 5th Int. Symp. Turb. Shear Flow Phenomena, Munich, Germany*, 2007.

[9] P. Spalart, S. Deck, M. Shur, K. Squires, M. Strelets, and A. Travin, "A new version of detached-eddy simulation, resistant to ambiguous grid densities," *Theor. Comput. Fluid Dyn.*, vol. 20, no. 3, pp. 181–195, 2006.

[10] T. Tran, *Développement d'une méthode hybride RANS-LES temporelle pour la simulation de sillages d'obstacles cylindriques*. PhD thesis, ENSMA, Poitiers, France, 2013.

[11] D. Lyn, S. Einav, W. Rodi, and J.-H. Park, "Laser-Doppler velocimetry study of ensemble-averaged characteristics of the turbulent near wake of a square cylinder," *J. Fluid Mech.*, vol. 304, pp. 285–319, 1995.

[12] Y. Cao and T. Tamura, "Large-eddy simulations of flow past a square cylinder using structured and unstructured grids," *Comput. Fluids*, vol. 137, pp. 36–54, 2016.

[13] M. Breuer, B. Jaffrézic, N. Peller, M. Manhart, J. Fröhlich, C. Hinterberger, W. Rodi, G. Deng, O. Chikhaoui, S. Jakirlić, *et al.*, "A comparative study of the turbulent flow over a periodic arrangement of smoothly contoured hills," in *Direct and Large-Eddy Simulation VI*, pp. 635–642, Springer, 2006.

[14] L. Thobois, G. Rymer, T. Soulères, and T. Poinsot, "Large-Eddy Simulation in IC Engine Geometries," in *2004 SAE Fuels & Lubricants Meeting & Exhibition*, SAE International, 2004.